FFI RAPPORT

Material properties of wolfram carbide established by using a simple indentation test

Moxnes John F, Nilssen Jan Rune, Friis Eva, Frøyland Øyvind

FFI/RAPPORT-2003/01429

FFIBM/860/01

Approved
Kjeller 20. November 2003

Bjarne Haugstad
Director of Research

MATERIAL PROPERTIES OF WOLFRAM CARBIDE ESTABLISHED BY USING A SIMPLE INDENTATION TEST

Moxnes John F, Nilssen Jan Rune, Friis Eva, Frøyland Øyvind

FFI/RAPPORT-2003/01429

FORSVARETS FORSKNINGSINSTITUTT
Norwegian Defence Research Establishment
P O Box 25, NO-2027 Kjeller, Norway

FORSVARETS FORSKNINGSINSTITUTT (FFI)
Norwegian Defence Research Establishment

P O BOX 25
N0-2027 KJELLER, NORWAY

UNCLASSIFIED

SECURITY CLASSIFICATION OF THIS PAGE (when data entered)

REPORT DOCUMENTATION PAGE

1) PUBL/REPORT NUMBER	2) SECURITY CLASSIFICATION	3) NUMBER OF PAGES
FFI/RAPPORT-2003/01429	UNCLASSIFIED	16
1a) PROJECT REFERENCE	**2a) DECLASSIFICATION/DOWNGRADING SCHEDULE**	
FFIBM/860/01	-	

4) TITLE

MATERIAL PROPERTIES OF WOLFRAM CARBIE ESTABLISHED BY USING A SIMPLE INDENTATION TEST

5) NAMES OF AUTHOR(S) IN FULL (surname first)

Moxnes John F, Nilssen Jan Rune, Friis Eva, Frøyland Øyvind

6) DISTRIBUTION STATEMENT

Approved for public release. Distribution unlimited. (Offentlig tilgjengelig)

7) INDEXING TERMS

IN ENGLISH:	IN NORWEGIAN:
a) Indentation	a) Innpressing
b) Hardness	b) Hardhet
c) Steel	c) Stål
d) Wolfram Carbide	d) Wolfram karbid
e)	e)

THESAURUS REFERENCE:

8) ABSTRACT

In this article a study of the fracture stress caused by indentation of wolfram carbide penetrators into steel blocks has been carried out. Experimental data was compared with simulations using the Nike-2D code and with numerical solutions from an analytical penetration theory.

We found that the Nike-2D simulations and the penetration model gave good agreement with experiments, and that an inverse modelling technique can be used to find the material properties of the penetrator.

9) DATE	AUTHORIZED BY	POSITION
20. November 2003	This page only Bjarne Haugstad	Director of Research

ISBN 82-464-0829-1

UNCLASSIFIED

SECURITY CLASSIFICATION OF THIS PAGE (when data entered)

CONTENTS

MATERIAL PROPERTIES OF WOLFRAM CARBIDE ESTABLISHED BY USING A SIMPLE COMPRESSION TEST

1 INTRODUCTION

Nammo Raufoss AS is the inventor of the Multipurpose (MP) ammunition concept. The MP technology was developed during the end of the 60s and the first series production started in the beginning of the 70s. Still the product is of great importance for the company's medium caliber division, and it is important to control and foresee the penetration capabilities of the MP round.

The hard-core of the 12.7 mm MP projectile consists of wolfram carbide. Shooting test at the firing range suggest that the yaw angle of the hard-core at impact is important for the penetration capabilities and the number of fragments behind armour. The penetration capabilities of the hard-core when impacting a target is of course strongly dependent on the material properties of the hard-core. The material properties are therefore necessary to establish before doing computer simulations.

In an earlier study, a bending test of the hard-core of the 12.7 mm MP round, made of wolfram carbide, has been carried out [1]. It was reason to believe that the fracture stress of the wolfram carbide during compression is much larger than predicted by tensile tests. This is a reasonable assumption since the tension test showed a brittle fracture, and a difference between the fracture stress in tension and compression (e.g. during penetration) is to be expected for brittle materials.

In order to analyze the fracture stress of wolfram carbide during compression an ordinary indentation test of the wolfram carbide penetrating into the steel block has been carried out. Simulation results from the Nike 2D [2] was compared with experimental results from the tension test and with numerical results from the standard theory of indentation (cavity theory) [3]. During indentation, the penetrator first penetrates the steel block. Thereafter, fracturing of the hard-core appears at a maximal axial force. Complete indentation of the penetrator nose into the target has not been possible to achieve so far.

2 THE EXPERIMENTAL SET-UP

In figure 2.1 the experimental set-up is shown

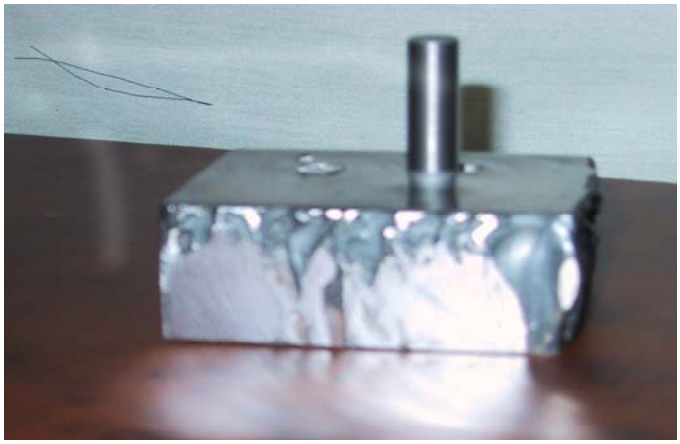

Figure 2.1 The experimental set-up

The experimental recording was the force and the displacement of the penetrator into the steel block. The rear part of the penetrator was mounted into a supportive block of the same steel quality as the steel block used for indentation. Regarding the penetrator, its length was reduced to avoid it to fracture due to bending as experienced in earlier indentation tests. The hard-core was pushed into the steel block at a rate of 2 mm/minute.

3 ANALYTICAL AND EXPERIMENTAL RESULTS

In this section obtained experiment results are compared with the analytical penetration theory and simulation. Figure 3.1 shows the Lagrange grid of the steel block and the Lagrange grid of the hard-core penetrator. Only the hard-core of the projectile is modelled since x-ray pictures and simulations show that only the hard-core of the projectile is able to penetrate into the steel target

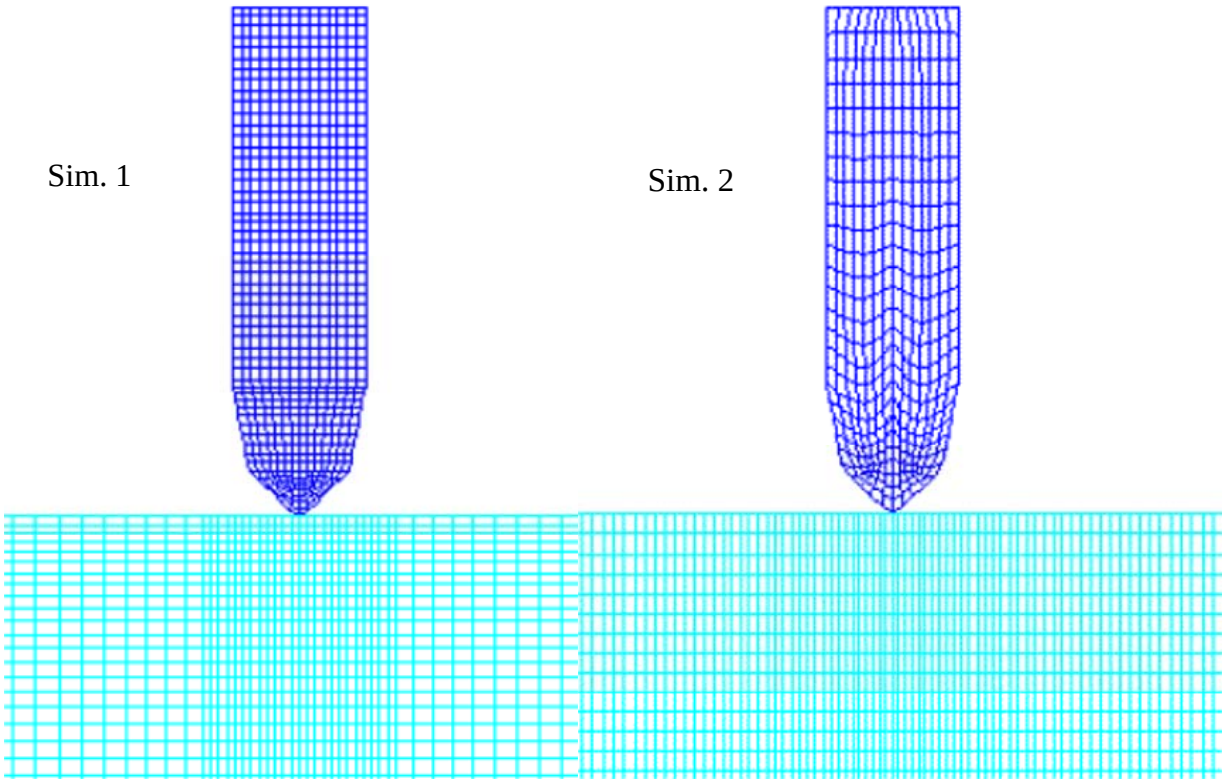

Sim. 3

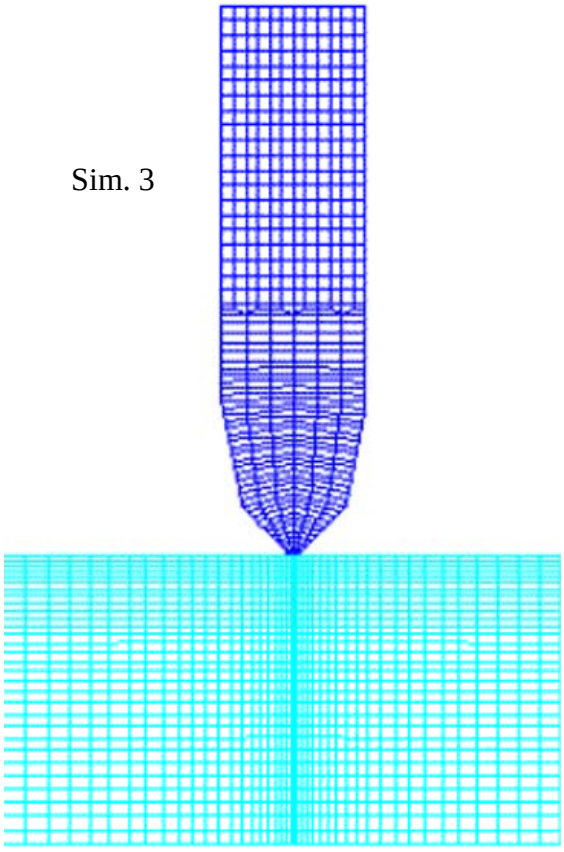

Figure 3.1: Different grid types used in Nike 2D.

The analytical cavity expansion theory gives that

$$F_e(d) = \frac{2}{3} Y_t (1 + Log[E_t / (3(1-\nu) Y_t)])[A_{p1}(d)(1 + \mu / Tan(\psi_1)) + A_{p2}(d)(1 + \mu / Tan(\psi_2))] \quad (3.1)$$

where A_{p1} and A_{p2} are the projected areas of the different conical parts that are in contact with the steel block, E_t is the Young's modulus of the target, Y_t is the yield stress of the target, μ is the coefficient of friction, ψ_1 is the half angle of the first conical part, ψ_2 is the half angle of the second conical part and d is the indentation depth. The friction coefficient between the hard-core and the steel block is 0.1 in the analytical theory.

Figure 3.2 and 3.3 show three different curves: The experimental forces and the analytical force from equation (3.1), all as a function of the penetration depth. The chosen material parameters are given in appendix A. Figure 3.3 is for the penetrator with a modified nose profile as shown in figure 3.7. Figure 3.4 and 3.5 show the true stress. True stress is defined as the force divided by the projected cross section area of the hard-core in contact with the steel block. This area is calculated according to the indentation depth.

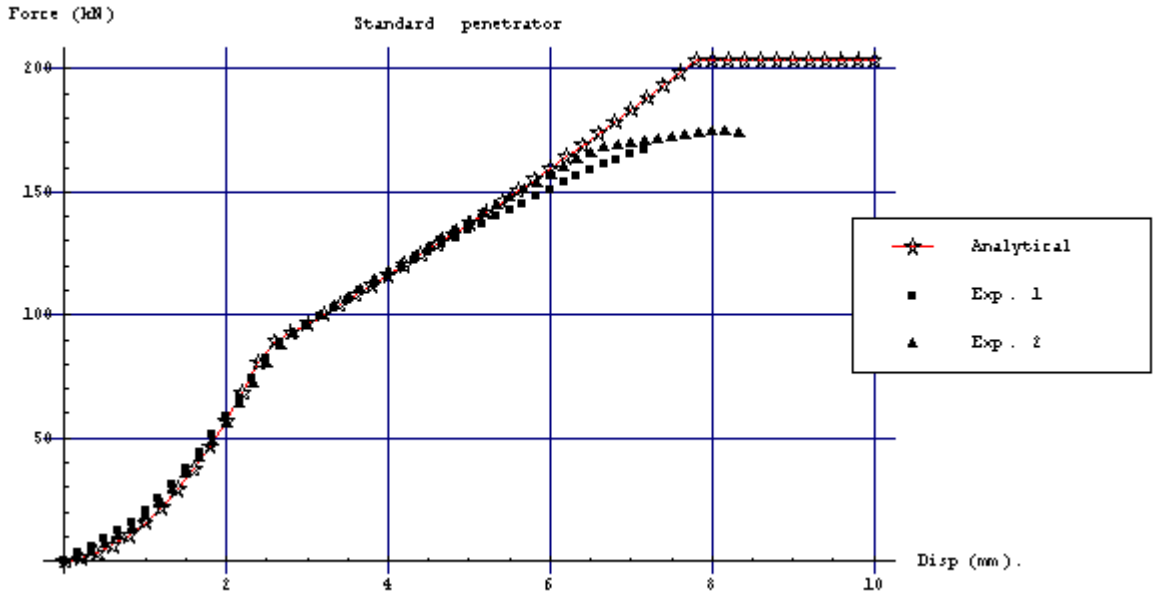

Figure 3.2: The force as a function of the indentation depth.

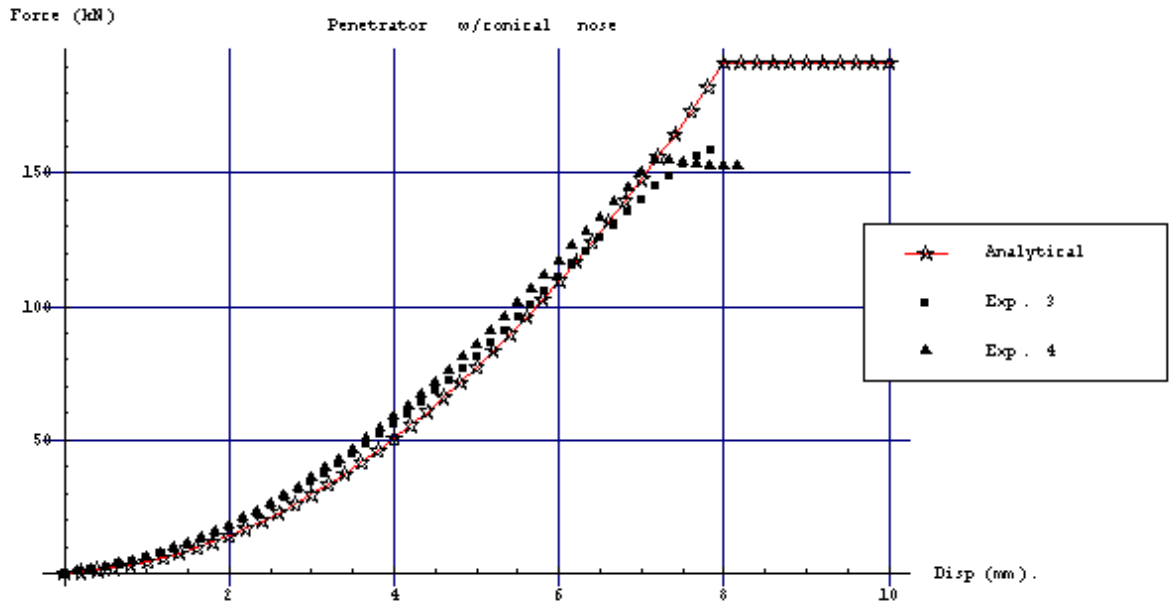

Figure 3.3: The force as a function of the indentation depth.

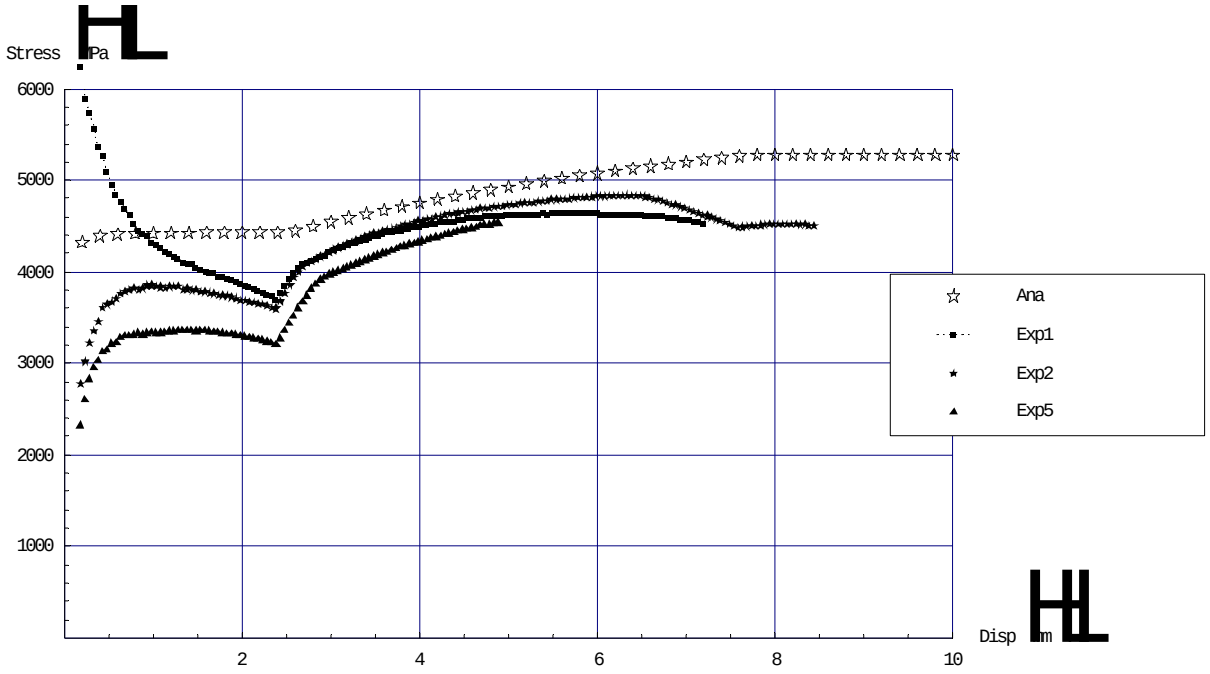

Figure 3.4: True stress as a function of indentation depth for the hard-core with standard nose profile.

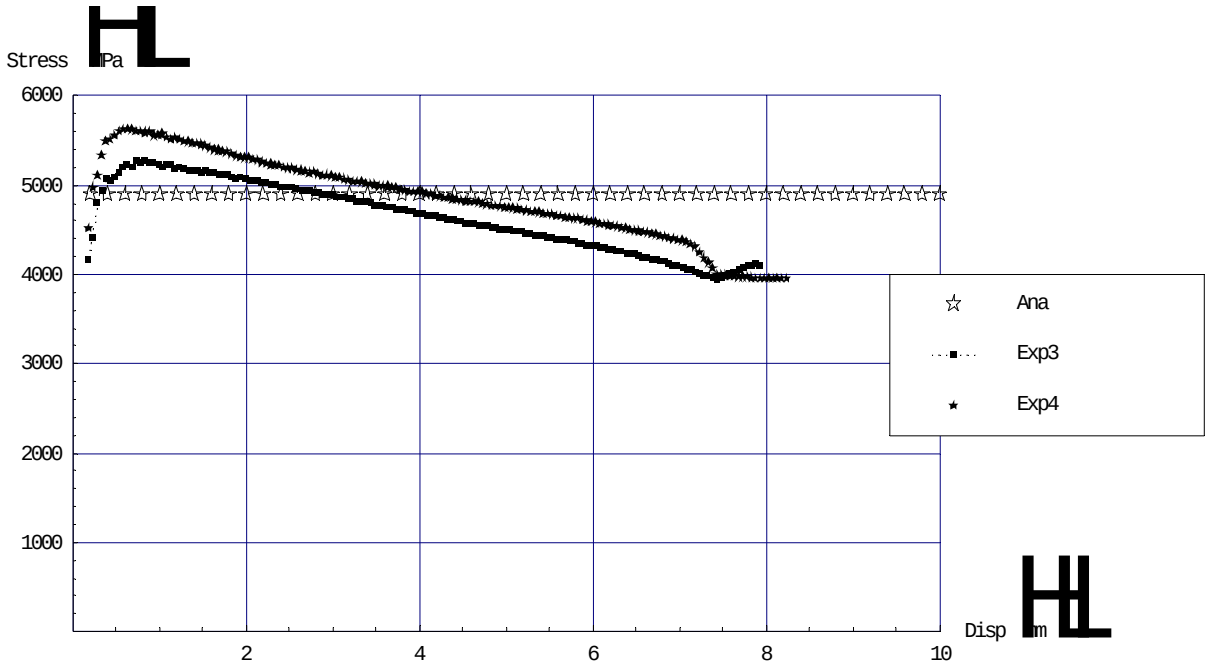

Figure 3.5: True stress as a function of indentation depth for the hard-core with conical nose profile.

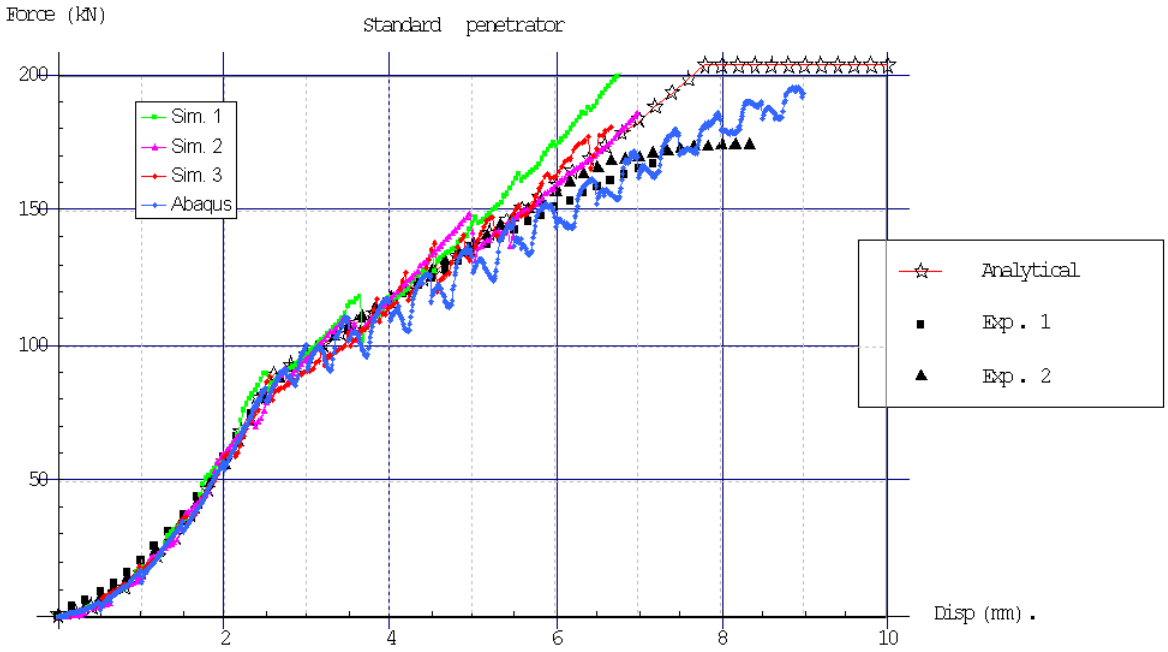

Figure 3.6: Simulations vs. experiments

We observe that the agreement between theory and experiments is fairly good, but at the end of the indentation there is a discrepancy between theory and experiments in figure 3.2 and 3.3. The explanation is that the support block yielded at this final stage of the indentation process. The analytical results in figure 3.4 show that the stress increases during penetration. The cause for this is that the friction comes more into consideration during the second phase of the penetration. The reason for the somewhat large scatter in the experimental results for the stress in figure 3.4 is related to the definition of the initial penetration of the hard core. Small differences in the initial penetration depth leads to large differences in the stress since the stress is calculated by dividing the force with the projected contact area. This “calibration” problem is also visible in figure 3.5 where the experimental stress seems to be varying with the depth of penetration.

The results from the simulations in Nike-2D are shown in figure 3.6. As we can see, they give fairly good agreement with the experimental results, although they show a more fluctuating force-indentation curve.

The radius along the longitudinal axis for the two different hard-core designs are shown in figure 3.7.

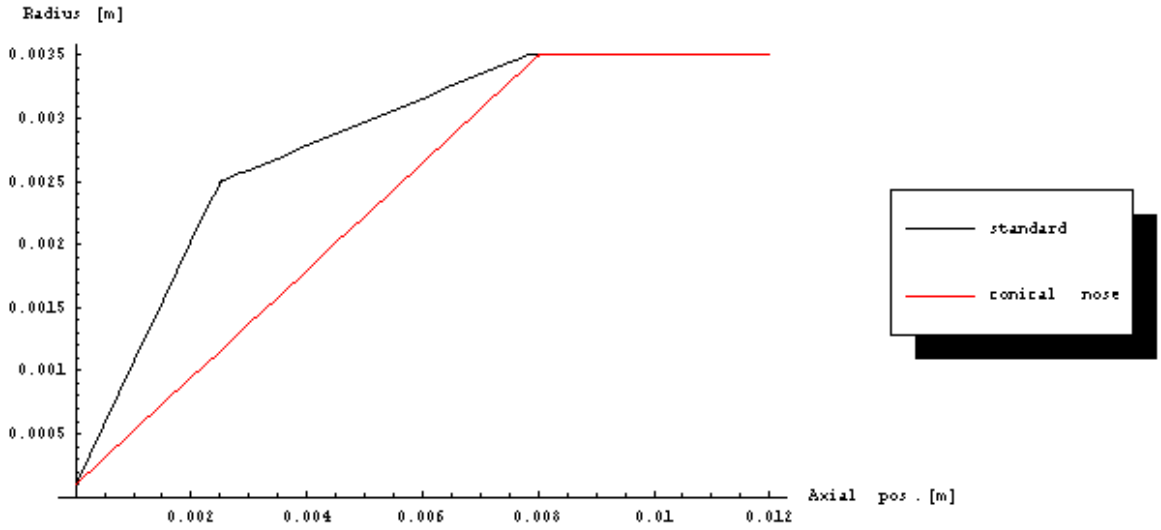

Figure 3.7: The radii of the hard-core as a function of the axial position

Tables (3.1) and (3.2) show the different tests results.

Test no.	Data at fracture/end point			
	Force [kN]	Indentation depth* [mm]	Radius** [mm]	Stress**** [GPa]
MX110403	152,65	5,898	3,141	4,93
MX130901	131,17	4,989	2,970	4,73
MX130903	152,87	5,444	3,055	5,21
MX130904	139,53	5.196	3.052	4.77
MX110901	168,72	7,500	3,442	4,53
MX110902	174,05	8,500	3,500	4,52
MX181205	160,32	6,898	3,329	4,60
MX181206	170,23	7,611	3,464	4,52
MX110903	158,23	7,993	3,497	4,12
MX110904	152,81	8,286	3,500	3,97
MX181204	79,58	2.147***	2,161	5,42

*Table 3.1 * Measured values.*
*** Radius of the cross section in contact with the target block is calculated from the measured indentation depth (column no. 3). There is discrepancy between the measured indentation depth and the actual indentation depth due to yield in the supportive steel block at the back end of the hard-core.*
**** This indentation depth was corrected and is not the measured value.*
***** Stress given as the force divided with the projected contact surface.*

Test no.	Comments
MX110403	Standard length of hard core, some bending was observed
MX130901	Exp. 5 in figures, Standard length of hard core, some bending was observed
MX130903	Standard length of hard core, some bending was observed
MX130904	Standard length of hard core, some bending was observed
MX110901	Exp. 1 in figures, length of hard-core reduced to 1.5 cm, did not fracture
MX110902	Exp. 2 in figures, length of hard-core reduced to 1.5 cm, did not fracture
MX181205	Harder support block was used, length of hard-core reduced to 1.5 cm
MX181206	Harder support block was used, length of hard-core reduced to 1.5 cm, new manufacturer
MX110903	Exp. 3 in figures, conical nose, length of hard-core reduced to 1.5 cm, did not fracture
MX110904	Exp. 4 in figures, conical nose, length of hard-core reduced to 1.5 cm, did not fracture
MX181204	Harder target and support block, length of hard-core reduced to 1.5 cm

Table 3.2

4 CONCLUSION/DISCUSSION

We found that the simulations and the analytical results show good agreement with the experimental results. Some of the compression tests lead to somewhat non-axial forces for the hard-core of standard length (ca. 8 cm). This was due to misalignment of the longitudinal axis of the hard-core with respect to the axis of compression. Therefore the length was shortened to 1.5 cm to reduce the effect of this phenomenon. We were not able to press the nose of the hard-core completely into the target. Even the nose section of the shortened hard-cores, of length 1.5 cm, did not come completely into the target. For Exp. 1 and Exp. 2 the support block yielded significantly, while MX181205 fractured somewhat near 7 mm of indentation. MX181204 fractured at a highest stress of 5.42 GPa. Thereby the results indicate some scattering in the material properties of the hard-core. Sandvik Hard Materials reports 5.2 GPa as compressive strength for our hard-core H10N. The experimental results for the true stress show some scattering for small penetration depth. This is due to the reasons mentioned in the previous section.

References

[1] Nilssen J.R., Moxnes J.F., Sagsveen B.A., Material properties of Wolfram Carbide established by using a bending test, FFI report-2002/02387

[2] Nike-2D user Manual

[3] Bishop R.F., Hill R., Mott N.F., The Theory of Indentation and Hardness Tests, Proc. Phys. Soc. Vol.57, Part 3, No. 321, pp. 147-159, May 1945

APPENDIX A

The following material parameters were used in the analytical theory:

Penetrator: (H10N)
Density: 14.55g/cm^3 (measured at FFI), 89-91% WC, 9-11% Co, C max 0.03%, Fe max 0.35%, Titan and Tantalum max 0.5%, Hardness 89 ±2 HRA,
Particle diameter: Less than 8 micron,
Tensile strength : 2.75GPA
Radius: 3.5 mm, Bending length: 1.0 cm
Sandvik Hard Materials report (H10N): Density: 14.25g/cm^3, Youngs modulus: E= 585 GPa, Poisson relation: 0.22, Compressive strength 5.2 GPA

Steel blocks:
Density: 7.9g/cm^3, Youngs modulus: E= 206 GPa, Poisson relation: 0.30
Yield strength: 1.1 GPa
Yield function (Elastic-Plastic, piece wise linear): Plastic Strain: 0.0, 0.05, 0.11, 0.2, 0.4, 0.6, 0.8, 1.0, 2.0, 3.5. Stress (GPa): 1.1,1.19, 1.224, 1.25, 1.3, 1.333, 1.371, 1.404, 1.584, 1.814.

Friction coefficient between steel and penetrator: 0.1. The analytical results were based on a elastic perfect plastic material with a yield strength of 1.1 GPa

DISTRIBUTION LIST

FFIBM **Dato:** 20. November 2003

RAPPORTTYPE (KRYSS AV)	RAPPORT NR.	REFERANSE	RAPPORTENS DATO
X RAPP ☐ NOTAT ☐ RR	2003/01429	FFIBM/860/01	20 November 2003
RAPPORTENS BESKYTTELSESGRAD		ANTALL EKS UTSTEDT	ANTALL SIDER
Unclassified		27	17
RAPPORTENS TITTEL		FORFATTER(E)	
MATERIAL PROPERTIES OF WOLFRAM CARBIDE ESTABLISHED BY USING A SIMPLE COMPRESSION TEST		Moxnes John F, Nilssen Jan Rune, Friis Eva, Frøyland Øyvind	
FORDELING GODKJENT AV FORSKNINGSSJEF		FORDELING GODKJENT AV AVDELINGSSJEF:	
Bjarne Haugstad		Jan Ivar Botnan	

EKSTERN FORDELING

ANTALL	EKS NR	TIL
1		Flo Land/AMM
1		Alf Øversveen Postboks 24 NO-2831 Raufoss
1		Nammo Raufoss AS
1		Eva Friis
1		Monica Strømgård
1		Knut Kristensen
1		Knut Rørhus
1		Gard Ødegårdstuen Postboks 162 NO-2831 Raufoss
1		Naval Air Warfare Center Weapons Division
1		Alice I. Atwood
1		Allen Lindfors Code 4T4310D 1 Administration Circle China Lake, CA 93555-6100
1		Dave Holt Naval Surface Warfare Center NAVAIR Medium Caliber Ammunition Crane Division Code 4022, Bldg 2540 300 Hwy 361 Crane, IN 47522-5011

INTERN FORDELING

ANTALL	EKS NR	TIL
2		FFI-Bibl
1		Adm direktør/stabssjef
1		FFIE
1		FFISYS
1		FFIBM
1		FFIN
2		Avd ktr, FFIBM
4		Forfattereksemplar(er)
		Elektronisk fordeling:
		FFI-veven
		Bjarne Haugstad, FFIBM Svein W Eriksen, FFIBM John F Moxnes, FFIBM Gunnar Ove Nevstad, FFIBM Jan Rune Nilssen, FFIFV Øyvind Frøyland, FFIBM

FFI-K1 Retningslinjer for fordeling og forsendelse er gitt i Oraklet, Bind I, Bestemmelser om publikasjoner for Forsvarets, pkt 2 og 5. Benytt ny side om nødvendig.